Pediatrics[1], Jining No. 1 People's Hospital, Jining City; Department of Pathology[2], The first 84 Hospital of the PLA, Yingtan City, P.R. China

Ibrutinib improves the development of acute lymphoblastic leukemia by activating endoplasmic reticulum stress-induced cell death

Zhaohui Li[1], Jia Wu[2], Lei Sheng[1,*]

Received January 5, 2018, accepted February 9, 2018

[*]Corresponding author: Dr. Lei Sheng, Pediatrics, Jining No. 1 People's Hospital, No. 6, Jining Health Road, Jining City, Shandong Province, 272000, P.R. China
ag20180104@yeah.net

Pharmazie 73: 294–299 (2018) *doi: 10.1691/ph.2018.8306*

The current study mainly aims to evaluate the effects of ibrutinib on endoplasmic reticulum stress (ERS)-induced apoptosis in Reh cells, which may shed light on the treatment of acute lymphoblastic leukemia (ALL) among children. In line with previous studies, our data show that ibrutinib significantly suppressed Reh cell viability in a time- and dose-dependent manner. We further evaluated the role of ibrutinib on Reh cell colony formation and apoptosis. Ibrutinib inhibited clonogenic capacity and induced Reh cell apoptosis, suggesting an anti-tumor effects of ibrutinib in the progression of ALL. Further study showed that ibrutinib treatment increased ERS-related protein expression, including Bip, ATF4 and CHOP, suggesting the induction of ER-stress in Reh cells. More importantly, once ER-stress was suppressed by tauroursodeoxycholic acid (TUDCA), an ER-stress inhibitor, the upregulation of Bip, ATF4, CHOP, cleaved-caspase3 and cleaved-PARP after ibrutinib treatment was partially reversed, suggesting that induction of ALL cell apoptosis by ibrutinib was partially attributed to activation of ER stress. In summary, we showed novel data that ER-stress induced cell apoptosis plays a key role in the therapeutic effects of ibrutinib on ALL cell malignancies.

1. Introduction

As an aggressive hematological malignancy, acute lymphoblastic leukemia (ALL) contributes to 25% of all childhood tumors (Gupta et al. 2016). In recent years, improved prognosis in childhood ALL has been widely achieved in both developed and developing countries (Matsunaga et al. 2012; Pastore and Levine 2015). Even though, the overall long-term survival of ALL patients is still wandering at about 30 % to 50 % and high risk of relapse is considered a major reason (National Comprehensive Cancer 2003; O'Donnell et al. 2017). Hence, it is important to further explore novel therapeutic approaches.

The endoplasmic reticulum (ER) is extensively involved in the regulation of multiple cellular processes, including protein folding and post-translational modification, thereby maintaining the intracellular homeostasis (Shi et al. 2016, Yu et al. 2016). In the circumstances of external stimuli, the unfolded protein response (UPR), mediated by three ER transmembrane protein sensors, including inositol-requiring enzyme 1α (IRE1α), double-stranded RNA dependent protein kinase-like ER kinase (PERK) and activating transcription factor 6 (ATF6), is initiated to restore intracellular homeostasis (Banerjee et al. 2016; Cerezo and Rocchi 2017). However, sustained ER-stress (ERS) would result in ERS-mediated cell apoptosis (Fujimoto et al. 2016). Accumulating evidences have shown that ERS-induced apoptosis plays an important role in the anti-tumor therapies (Lin et al. 2013).

Ibrutinib (Imbruvica), formerly known as PCI-32765, selectively and irreversibly inhibits Bruton's tyrosine kinase (BTK), a key enzyme in B-cell receptor signaling pathway (Castillo et al. 2016; Filanovsky and Shvidel 2017). Recently, ibrutinib has been approved by the U.S. Food and Drug Administration and European Medicines Agency, and is widely applied for the therapy of patients with lymphoproliferative disorders, including mantle cell lymphoma, chronic lymphocytic leukemia, and ALL (Muschen 2015; Long et al. 2017). However, the specific underlying mechanism has been poorly understood.

In the current study, we mainly evaluated the effects of ibrutinib on ERS-induced apoptosis in Reh cells, which may shed light on the treatment of ALL among children.

2. Investigations and results

2.1. Ibrutinib suppresses Reh cell viability and colony formation capacity

First, we treated Reh cells with 0.25, 1, 5, 10 and 25 μM for 48 h. CCK-8 assay indicated that Reh cell viability was decreased in a dose-dependent manner after ibrutinib treatment (Fig. 1A). Additionally, Reh cells were treated with 10 μM ibrutinib for 24, 48, 72 h, respectively. Our data showed that Reh cell viability was decreased to 67.5 %, 52.3 %, and 41.3 %, respectively (Fig. 1B). Besides, we also investigated the clonogenic capacity after ibrutinib treatment. As shown in Fig. 3C, treatment with 5, 10 and 25 μM ibrutinib for 48 h significantly reduced the clone formation capacity. These data indicated strong anti-tumor effects of ibrutinib in ALL cell lines.

2.2. Ibrutinib enhances Reh cell apoptosis

Furthermore, flow cytometry was carried out to evaluate the effects of ibrutinib on Reh cell apoptosis. Our data showed that treatment with 10 μM ibrutinib for 48 h significantly enhanced Reh cell apoptosis rate by ~4.25-fold (Fig. 2A). TUNEL staining also demonstrated increased apoptotic cells after 10 μM ibrutinib incubation for 48 h (Fig. 2B). Western blot assay showed that the protein levels of apoptosis markers, including cleaved-caspase3 and cleaved poly ADP-ribose polymerase (PARP), were upregulated after 10μM ibrutinib treatment (Fig. 2C).

2.3. Ibrutinib induces ER-stress in Reh cells

Then, we evaluated whether 10 μM ibrutinib treatment could induce ERS in Reh cells. Real time PCR analysis showed that

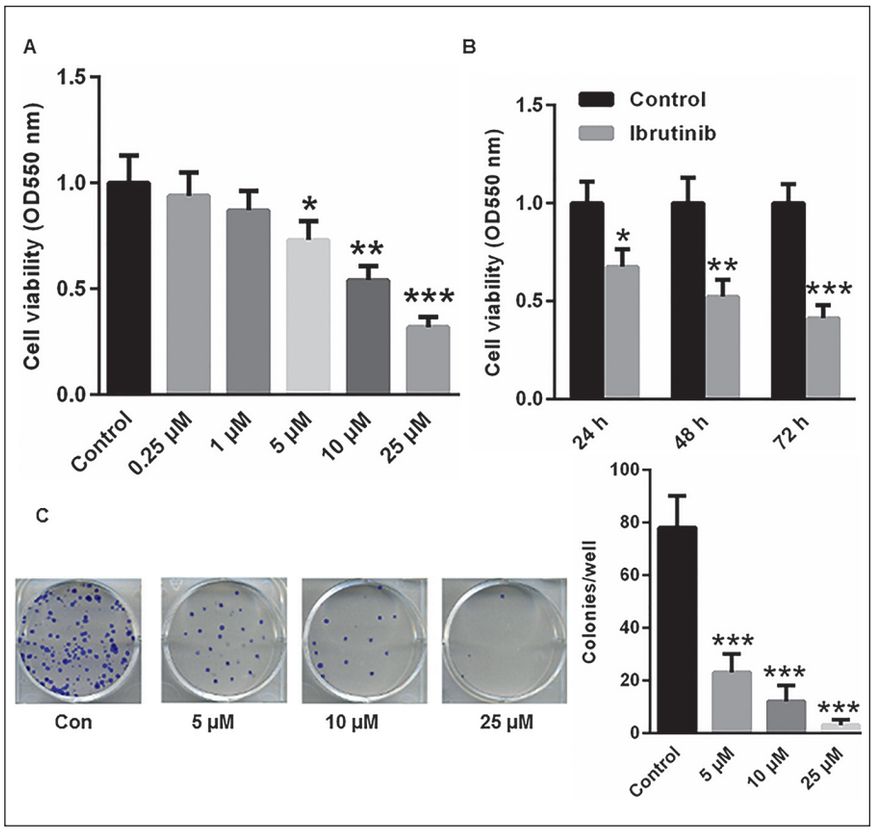

Fig. 1: Ibrutinib exerted strong anti-tumor effects in Reh cells. (A) CCK-8 assay indicated that Reh cell viability was decreased in a dose- dependent manner after ibrutinib treatment. (B) Reh cell viability was decreased to 67.5 %, 52.3 %, 41.3 %, respectively. (C) Treatment with 5, 10 and 25 μM ibrutinib for 48 h significantly reduced the clone formation capacity. $^{*}p<0.05$, $^{**}p<0.01$, $^{***}p<0.001$ vs. control.

ibrutinib significantly increased the mRNA levels of Bip, ATF4 and CHOP (Fig. 3A). Meanwhile, western blot assay showed that the protein levels of Bip, ATF4 and CHOP were also increased in Reh cells after 10μM ibrutinib treatment (Fig. 3B).

2.4. Ibrutinib increased Reh cell apoptosis via activating ERS

To further evaluate whether ibrutinib induced Reh cell apoptosis was mediated *via* ER-stress, Reh cells were preincubated with 5 μM tauroursodeoxycholic acid (TUDCA), an inhibitor of ERS, in the presence or absence of ibrutinib. Compared with control, treatment with TUDCA significantly decreased the mRNA levels of ERS markers, including Bip, ATF4 and CHOP (Fig. 4A). However, ibrutinib-induced upregulation of Bip, ATF4 and CHOP could largely be abolished by TUDCA preincubation (Fig. 4A). Meanwhile, we also analyzed the expression of Bip, ATF4, CHOP, cleaved-caspase3 and cleaved-PARP. Our data showed that TUDCA treatment significantly reduced the levels of Bip, ATF4, CHOP, cleaved-caspase3 and cleaved-PARP (Fig. 4B). More importantly, increased expression of Bip, ATF4, CHOP, cleaved-caspase3 and cleaved-PARP after ibrutinib treatment could be largely relieved by TUDCA treatment (Fig. 4B). These data demonstrated that ibrutinib-induced Reh cell apoptosis was partially mediated via ER-stress.

3. Discussion

ALL is the most common pediatric cancer and is estimated to account for ~25% of all malignancies among children younger than 15 years (Gupta et al. 2016). Recent progress in chemotherapy and supportive care has markedly decreased ALL-related mortality (Cagnetta et al. 2015; Lamothe et al. 2016). However, relapse and recurrent ALL is a still major reason for the cure rate and mortality among children with ALL malignancies.

A variety of drugs have been widely used for the therapy of ALL (Winqvist et al. 2016). As a first-in-class oral covalent inhibitor of Bruton's tyrosine kinase (BTK), ibrutinib has been approved for the therapy of patients with chronic lymphocytic leukemia (CLL) (Vela et al. 2016; Wanquet et al. 2016). It is found that ibrutinib can significantly suppress CLL cell survival and proliferation via interacting with B-cell receptor and chemokine receptors (Vela et al. 2016; Wanquet et al. 2016). Recently, ibrutinib is also shown to be effective in suppressing ALL cell proliferation and viability (Rotin et al. 2016a,b).

In line with previous studies, our data showed that ibrutinib significantly suppressed Reh cell viability in a time- and dose-dependent manner. We further evaluated the role of ibrutinib on Reh cell colony formation and apoptosis. Our data showed that ibrutinib inhibited clonogenic capacity and induced Reh cell apoptosis, suggesting the anti-tumor effects of ibrutinib in the progression of ALL.

These above observations prompted us to further elucidate the underlying mechanism by which ibrutinib inhibits the survival and proliferation of Reh cells in the progression of ALL. Unfolded protein response (UPR) is an important ER stress pathway, and is considered to restore ER homeostasis thereby maintaining cell survival (Fruci et al. 2006; Chen et al. 2012). However, uncontrollable and excessive ER damage is suggested to induce cell death (Hu et al. 2015; Lamothe et al. 2016). Several studies have shown that multiple chemotherapeutic candidates could induce ER stress-related cancer cell death, thereby exerting anti-cancer effect (Rosati et al. 2013; Wang et al. 2016).

Hence, we tried to evaluate whether ibrutinib could induce ERS-related ALL cell death. Ibrutinib significantly induced Reh cancer cell apoptosis. Further study showed increased ERS-related protein expression, including Bip, ATF4 and CHOP, suggesting the induction of ER-stress in Reh cells after ibrutinib treatment. More importantly, once ER-stress was suppressed by TUDCA, an ER-stress inhibitor, the upregulation of Bip, ATF4, CHOP, cleaved-caspase3 and cleaved-PARP after ibrutinib treatment was partially reversed, suggesting that induction of ALL cell apoptosis by ibrutinib was partially attributed to activation of ER stress.

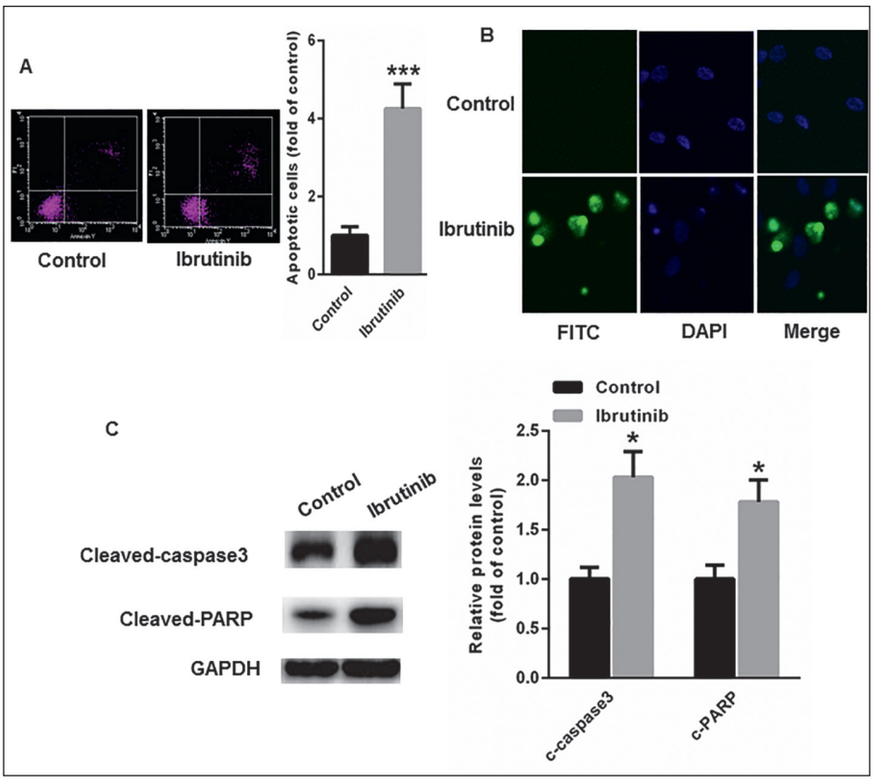

Fig. 2: Ibrutinib induced Reh cell apoptosis. (A) Treatment with 10 μM ibrutinib for 48 h significantly enhanced Reh cell apoptosis rate by ~4.25-fold. (B) TUNEL staining also demonstrated increased apoptotic cells after 10 μM ibrutinib incubation for 48 h. (C) The protein levels of cleaved-caspase3 and cleaved-PARP were upregulated after 10 μM ibrutinib treatment. $^{*}p<0.05$, $^{**}p<0.01$, $^{***}p<0.001$ vs. control.

In summary, for the first time, we showed that ER-stress induced cell apoptosis plays a key role in the therapeutic effects of ibrutinib on ALL cell malignancies. These findings may shed light on the treatment of ALL, thereby enhancing its anti-cancer efficacy in ALL patients.

4. Experimental

4.1. Cells and reagent

Human precursor-B ALL cell line, Reh, was purchased from American Type Culture Collection ATCC (CRL-8286). Cells were maintained in RPMI medium (Hyclone; GE Healthcare Life Sciences) supplemented with 10% fetal bovine serum (Hyclone;

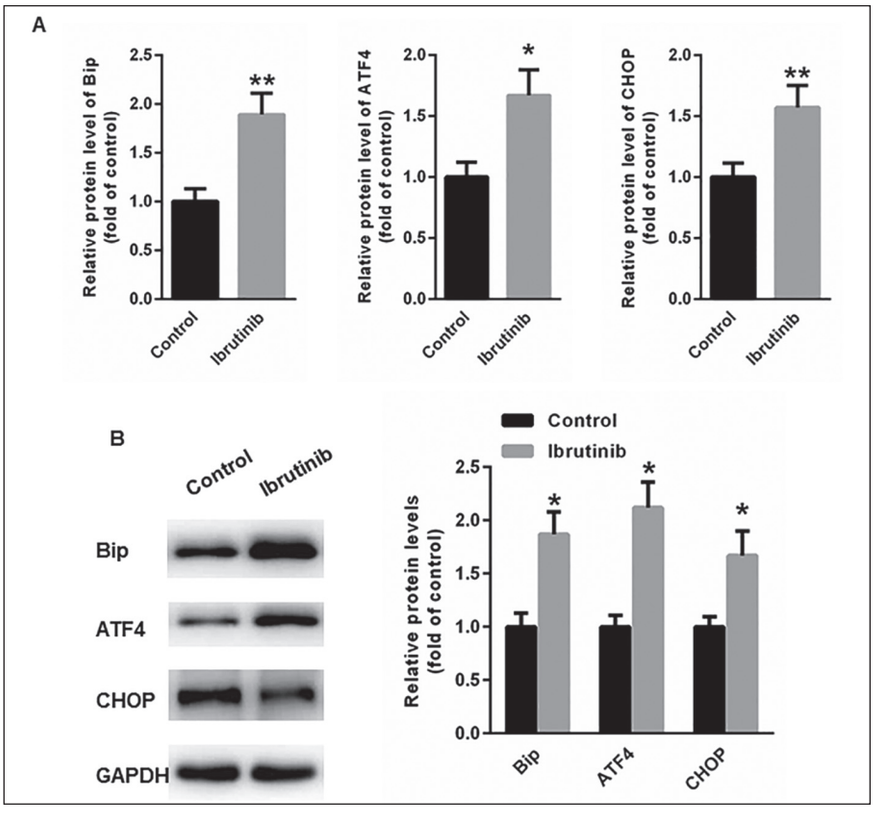

Fig. 3: Ibrutinib induced ER-stress in Reh cells. (A) Real time PCR analysis showed that ibrutinib significantly increased the mRNA levels of Bip, ATF4 and CHOP. (B) Western blot assay showed that the protein levels of Bip, ATF4 and CHOP were also increased in Reh cells after 10μM ibrutinib treatment. $^{*}p<0.05$, $^{**}p<0.01$, $^{***}p<0.001$ vs. control.

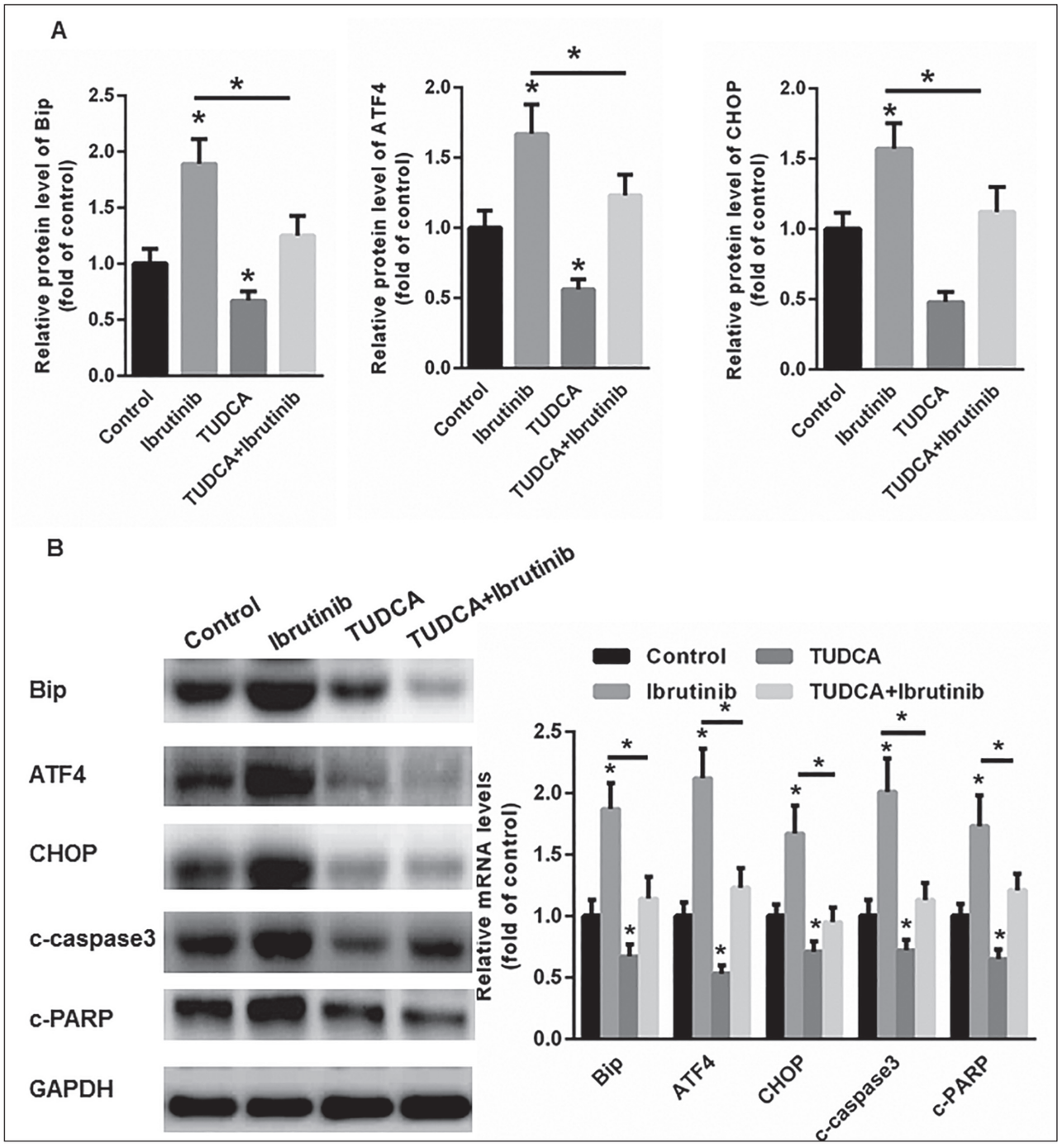

Fig. 4: Ibrutinib increased Reh cell apoptosis via activating ERS. (A) Real time PCR assay showed that ibrutinib-induced upregulation of Bip, ATF4 and CHOP mRNA levels could largely be abolished by TUDCA preincubation. (B) Increased expression of Bip, ATF4, CHOP, cleaved-caspase3 and cleaved-PARP after ibrutinib treatment could be largely relieved by TUDCA treatment. $^{*}p<0.05$, $^{**}p<0.01$, $^{***}p<0.001$ vs. control.

GE Healthcare Life Sciences) at 37 ˚C in a humidified atmosphere containing 5% CO_2. Ibrutinib (Sigma) was dissolved in DMSO (Sigma) and stored as a 10mM stock solution at -20 °C. Tauroursodeoxycholic acid (TUDCA) (Calbiochem) was stored as 1 M in DMSO (Sigma) at -20 °C.

4.2. Cell viability assay

Reh cells were seeded into 96-well plates at the density of 1×10^4 cells/well and cultured for 24 h. After that, ibrutinib was added to the wells at a final concentration of 0, 0.25, 1, 5, 10 and 25 μM for 48 h, and wells with equimolar DMSO were used as controls. Then, the CCK-8 solution (CA1210, Solarbio, Beijing, China) was added to each well following incubation for 40 min at 37 °C. Absorbance was determined at 450 nm using a spectrophotometer. For the time course cell viability assay, Reh cells were treated with DMSO, or 10 μM ibrutinib alone, or 2 mM TUDCA was added 40 min before ibrutinib. All experiments were performed in triplicate.

4.3. Clonogenic survival assay

Cells were suspended in 0.3% agar (Sigma-Aldrich, St. Louis, MO, USA) in culture medium with or without10 μM ibrutinib treatment for 48 h and plated at a density of 1×105 cells/dish into a 10 cm dish, which was preloaded with a thin layer of 1.0% agar. Cells were kept in media during the assay and monitored for colony formation. After culturing for 7 days, the colony formation was observed. The clones were stained with trypan blue (Sigma-Aldrich, St. Louis, MO, USA) to evaluate colony formation. Cells were subsequently imaged under a light microscope (40×, Olympus Corporation, Tokyo, Japan) and 10 individual fields were randomly chosen and counted per insert. The results are presented as the mean of three separate experiments.

4.4. Cell apoptosis assay

Following 10 μM ibrutinib or DMSO control treatment for 48 h, the cells were washed three times with cold phosphate-buffered saline (PBS). An Annexin V-fluorescein

isothiocyanate (FITC)-propidium iodide (PI) Apoptosis kit (Invitrogen; Thermo Fisher Scientific, Inc.) was used to measure cell apoptosis. Briefly, Reh cells were washed three times with 1x PBS and suspended at a density of 2-3x106 cells/ml in 1x Annexin-V binding buffer (10 mM HEPES/NaOH, pH 7.4, 140 mM NaCl, 2.5 mM $CaCl_2$). Annexin V-FITC and PI buffer were administered to the cells, which were then incubated for 15 min at room temperature in the dark. Cells lacking treatment with curcumin were used as an internal control. Following incubation, the cells were filtered with a 200 mesh filter screen and analyzed with a FACScan flow cytometer (BD FacsAria Fluidics Cart, BD Biosciences, San Jose, CA, USA) within 1 h of staining. And cell apoptosis was analyzed using *BDCellQuest* Pro Software (BD Biosciences, San Jose, CA, USA). A total of 10,000 cells were evaluated in each sample.

4.5. TUNEL assay

Nuclear fragmentation was detected using TUNEL staining with an apoptosis detection kit (R&D Systems, Inc., Minneapolis, MN, USA) according to the manufacturer's protocol. The cells were observed with fluorescence microscopy (Olympus).

4.6. Fluorescence microscopy

Reh cells were seeded on sterilized coverslips, were fixed in 4% phosphate-buffered neutral formalin at room temperature for 20 min. Sections were subsequently incubated with 0.3 % hydrogen peroxide/phosphate-buffered saline for 30 min. The sections were incubated with primary antibodies, Bip, ATF4, CHOP, cleaved-caspase3 and cleaved-PARP, (1:100, ab125020, Abcam, Cambridge, UK) at a 1:50 dilution and 4 ˚C overnight. Following washing with PBS three times for 5 min, the slides were blocked with 8 % albumin bovine serum (BSA; Sigma-Aldrich; Merck KGaA, Darmstadt, Germany) at room temperature for 2 h. After that the slides were washed with PBS for three times and incubated with tetramethylrhodamine-conjugated anti-rabbit immunoglobulin G (1:500; ZDR5209, Zhongshan Gold Bridge Co., Beijing, China) and with DAPI (1:1,000; C0060, Solarbio co., Beijing, China) for 20 min at room temperature. Following incubation with the secondary antibody, the slides were washed three times with PBS in the dark and the coverslips were mounted with a mounting medium and coated on glass slides. The slides were sealed at room temperature for ~1 h in the dark and fluorescence intensity was examined using a fluorescence microscope.

4.7. Real-time PCR analysis

The total RNA from Reh cells was isolated using TRIzol (Invitrogen; Thermo Fisher Scientific, Inc., Waltham, MA, USA) according to the manufacturer's protocol. The total RNA was reverse transcribed into cDNA using a TaqMan RNA Reverse Transcription kit (Applied Biosystems; Thermo Fisher Scientific, Inc.). qPCR was performed using SYBR Green Supermix (Bio-Rad Laboratories, Inc., Hercules, CA, USA) in a Bio-Rad iCycleriQ real-time PCR detection system as described above (Guo et al. 2014). GAPDH was used as an internal control. The primers used were listed as follows: GAPDH-F: 5`-GGAGCGAGATCCCTCCAAAAT-3`; GAPDH-R: 5`-GGCTGTTGTCATACTTCTCATGG-3`; Bip-F: 5`-TGACATTGAAGACTTCAAAGCT-3`; Bip-R: 5`-CTGCTGTATCCTCTTCACCAGT-3`; ATF4-F: 5`-GCTAAGGCGGGCTCCTCCGA-3`; ATF4-R: 5`-ACCCAACAGGGCATCCAAGTCG-3`; CHOP-F: 5`-GGAGCATCAGTCCCCCACTT-3`; HOP-R: 5`-TGTGGGATTGAGGGTCACATC-3`.

4.8. Immunoblot analysis

Proteins samples were extracted from Reh cells in radioimmunoprecipitaion assay buffer (1 % TritonX-100, 15 mmol/l NaCl, 5 mmol/l EDTA and 10 mmol/L Tris-HCl; pH 7.0; Beijing Solarbio Science & Technology Co., Ltd., Beijing, China) supplemented with a protease and phosphatase inhibitor cocktail (Sigma-Aldrich; Merck KGaA, Darmstadt, Germany). A bicinchoninic protein assay kit (Pierce; Thermo Fisher Scientific, Inc.) was used to determine the protein concentration. Equal quantities of protein (15 μg) separated by 10% SDS-PAGE and electrophoretically transferred to a PVDF membrane. Following blocking with 8% milk in PBS with Tween-20 (pH 7.5) for 2 h at room temperature, membranes were incubated with the following primary antibodies at 4 °C overnight: anti-GRP78/BiP (Cell Signaling, 3177); anti-IRE1α (Cell Signaling, 3294); anti-p-IRE1 (Abcam, 124945); anti-PERK (ab79483), anti-XBP1s (Cell Signaling, 12782); anti-cleaved PARP (Cell Signaling, 5625); anti-cleaved caspase-3 (Cell Signaling, 9664); anti-LC3B (Cell Signaling, 3868); anti-Beclin1 (Abcam, 207612) and β-actin (Santa Cruz, 70319) at a 1:1000 dilution. Following several washes with TBST, the membranes were incubated with HRP-conjugated goat anti-rabbit IgG (1:5,000; ZB-2306, Zhongshan Gold Bridge Biological Technology Co., Beijing, China) for 2 h at room temperature and then washed. The proteins were detected using enhanced chemiluminescence, according to the manufacturer's protocol (Merck KGaA, Darmstadt, Germany). ImageJ 1.8.0 (National Institutes of Health, Bethesda, MD, USA) was applied to quantify the relative protein levels. GAPDH was used as an internal control.

4.9. Statistical analysis

Data are presented as the mean±standard deviation for the indicated number of separate experiments. Three independent experiments were carried out for each study. Differences in the quantitative data between two groups were determined using the unpaired Student's *t*-test (GraphPad 6.0, Inc., LaJolla, CA, USA). Comparisons of means among multiple groups were determined using one-way analysis of variance (GraphPad 6.0, Inc., LaJolla, CA, USA). $P<0.05$ was considered to indicate a statistically significant difference.

Conflicts of interest: None declared.

References

Banerjee A, Ahmed H, Yang P, Czinn SZ, Blanchard TG (2016) Endoplasmic reticulum stress and IRE-1 signaling cause apoptosis in colon cancer cells in response to andrographolide treatment. Oncotarget 7: 41432-41444.

Cagnetta A, Caffa I, Acharya C, Soncini D, Acharya P, Adamia S, Pierri I, Bergamaschi M, Garuti A, Fraternali G, Mastracci L, Provenzani A, Zucal C, Damonte G, Salis A, Montecucco F, Patrone F, Ballestrero A, Bruzzone S, Gobbi M, Nencioni A, Cea M (2015) APO866 increases antitumor activity of cyclosporin-A by inducing mitochondrial and endoplasmic reticulum stress in leukemia cells. Clin Cancer Res 21: 3934-3945.

Castillo JJ, Treon SP, Davids MS (2016) Inhibition of the bruton tyrosine kinase pathway in B-Cell lymphoproliferative disorders. Cancer J 22: 34-39.

Cerezo M, Rocchi S (2017) New anti-cancer molecules targeting HSPA5/BIP to induce endoplasmic reticulum stress, autophagy and apoptosis. Autophagy 13: 216-217.

Chen J, Wei H, Xie B, Wang B, Cheng J, Cheng J (2012) Endoplasmic reticulum stress contributes to arsenic trioxide-induced apoptosis in drug-sensitive and -resistant leukemia cells. Leuk Res 36: 1526-1535.

Filanovsky K, Shvidel L (2017) Safety and efficacy of ibrutinib in a patient with severe renal impairment. Hematol Rep 9: 7078.

Fruci D, Ferracuti S, Limongi MZ, Cunsolo V, Giorda E, Fraioli R, Sibilio L, Carroll O, Hattori A, van Endert PM, Giacomini P (2006) Expression of endoplasmic reticulum aminopeptidases in EBV-B cell lines from healthy donors and in leukemia/lymphoma, carcinoma, and melanoma cell lines. J Immunol 176: 4869-4879.

Fujimoto A, Kawana K, Taguchi A, Adachi K, Sato M, Nakamura H, Ogishima J, Yoshida M, Inoue T, Nishida H, Tomio K, Yamashita A, Matsumoto Y, Arimoto T, Wada-Hiraike O, Oda K, Nagamatsu T, Osuga Y, Fujii T (2016) Inhibition of endoplasmic reticulum (ER) stress sensors sensitizes cancer stem-like cells to ER stress-mediated apoptosis. Oncotarget 7: 51854-51864.

Guo J, Li M, Meng X, Sui J, Dou L, Tang W, Huang X, Man Y, Wang S, Li J (2014) MiR-291b-3p induces apoptosis in liver cell line NCTC1469 by reducing the level of RNA-binding protein HuR. Cell Physiol Biochem 33: 810-822.

Gupta R, Chandgothia M, Dahiya M, Bakhshi S, Sharma A, Kumar L (2016) Multidrug resistance protein 1 as prognostic biomarker in clinical practice for acute myeloid leukemia. Int J Lab Hematol 38: e93-97.

Hu C, Xu M, Qin R, Chen W, Xu X (2015) Wogonin induces apoptosis and endoplasmic reticulum stress in HL-60 leukemia cells through inhibition of the PI3K-AKT signaling pathway. Oncol Rep 33: 3146-3154.

Lamothe B, Wierda WG, Keating MJ, Gandhi V (2016) Carfilzomib triggers cell death in chronic lymphocytic leukemia by inducing proapoptotic and endoplasmic reticulum stress responses. Clin Cancer Res 22: 4712-4726.

Lin S, Zhang J, Chen H, Chen H, Lai F, Luo J, Wang Z, Bu H, Zhang R, Li H, Tong H (2013) Involvement of endoplasmic reticulum stress in capsaicin-induced apoptosis of human pancreatic cancer cells. Evid Based Complement Alternat Med 2013: 629750.

Long M, Beckwith K, Do P, Mundy BL, Gordon A, Lehman AM, Maddocks KJ, Cheney C, Jones JA, Flynn JM, Andritsos LA, Awan F, Fraietta JA, June CH, Maus MV, Woyach JA, Caligiuri MA, Johnson AJ, Muthusamy N, Byrd JC (2017) Ibrutinib treatment improves T cell number and function in CLL patients. J Clin Invest 127: 3052-3064.

Matsunaga T, Yamashita K, Kubuki Y, Toyama T, Imataki O, Maeda K, Kawano N, Satou S, Kawano H, Ishizaki J, Yoshida S, Kameda T, Sasaki T, Sekine M, Kamiunten A, Taniguchi Y, Hidaka T, Katayose K, K-Shimoda H, Shide K, Yamamoto S, Moritake H, Nunoi H, Makino S, Kitanaka A, Matsuoka H, Shimoda K (2012) Acute myeloid leukemia in clinical practice: a retrospective population-based cohort study in Miyazaki Prefecture, Japan. Int J Hematol 96: 342-349.

Muschen M (2015) Rationale for targeting the pre-B-cell receptor signaling pathway in acute lymphoblastic leukemia. Blood 125: 3688-3693.

National Comprehensive Cancer N (2003) Acute myeloid leukemia. Clinical practice guidelines in oncology. J Natl Compr Canc Netw 1: 520-539.

O'Donnell MR, Tallman MS, Abboud CN, Altman JK, Appelbaum FR, Arber DA, Bhatt V, Bixby D, Blum W, Coutre SE, De Lima M, Fathi AT, Fiorella M, Foran JM, Gore SD, Hall AC, Kropf P, Lancet J, Maness LJ, Marcucci G, Martin MG, Moore JO, Olin R, Peker D, Pollyea DA, Pratz K, Ravandi F, Shami PJ, Stone RM, Strickland SA, Wang ES, Wieduwilt M, Gregory K, Ogba N (2017) Acute myeloid leukemia, version 3.2017, NCCN Clinical Practice Guidelines in Oncology. J Natl Compr Canc Netw 15: 926-957.

Pastore F, Levine RL (2015) Next-generation sequencing and detection of minimal residual disease in acute myeloid leukemia: ready for clinical practice? JAMA 314: 778-780.

Rosati E, Sabatini R, De Falco F, Del Papa B, Falzetti F, Di Ianni M, Cavalli L, Fettucciari K, Bartoli A, Screpanti I, Marconi P (2013) Gamma-secretase inhibitor I induces apoptosis in chronic lymphocytic leukemia cells by proteasome inhibition, endoplasmic reticulum stress increase and notch down-regulation. Int J Cancer 132: 1940-1953.

Rotin LE, Gronda M, Hurren R, Wang X, Minden MD, Slassi M, Schimmer AD (2016a) Investigating the synergistic mechanism between ibrutinib and daunorubicin in acute myeloid leukemia cells. Leuk Lymphoma 57: 2432-2436.

Rotin LE, Gronda M, MacLean N, Hurren R, Wang X, Lin FH, Wrana J, Datti A, Barber DL, Minden MD, Slassi M, Schimmer AD (2016b) Ibrutinib synergizes with poly(ADP-ribose) glycohydrolase inhibitors to induce cell death in AML cells via a BTK-independent mechanism. Oncotarget 7: 2765-2779.

Shi WY, Cao C, Liu L (2016) Interferon alpha Induces the Apoptosis of Cervical Cancer HeLa Cells by Activating both the Intrinsic Mitochondrial Pathway and Endoplasmic Reticulum Stress-Induced Pathway. Int J Mol Sci 17.

Vela CM, McBride A, Jaglowski SM, Andritsos LA (2016) Ibrutinib for treatment of chronic lymphocytic leukemia. Am J Health Syst Pharm 73: 367-375.

Wang J, Wang QL, Nong XH, Zhang XY, Xu XY, Qi SH, Wang YF (2016) Oxalicumone A, a new dihydrothiophene-condensed sulfur chromone induces apoptosis in leukemia cells through endoplasmic reticulum stress pathway. Eur J Pharmacol 783: 47-55.

Wanquet A, Birsen R, Lemal R, Hunault M, Leblond V, Aurran-Schleinitz T (2016) Ibrutinib responsive central nervous system involvement in chronic lymphocytic leukemia. Blood 127: 2356-2358.

Winqvist M, Asklid A, Andersson PO, Karlsson K, Karlsson C, Lauri B, Lundin J, Mattsson M, Norin S, Sandstedt A, Hansson L, Osterborg A (2016) Real-world results of ibrutinib in patients with relapsed or refractory chronic lymphocytic leukemia: data from 95 consecutive patients treated in a compassionate use program. A study from the Swedish Chronic Lymphocytic Leukemia Group. Haematologica 101: 1573-1580.

Yu XS, Du J, Fan YF, Liu FJ, Cao LL, Liang N, Xu DG, Zhang JD (2016) Activation of endoplasmic reticulum stress promotes autophagy and apoptosis and reverses chemoresistance of human small cell lung cancer cells by inhibiting the PI3K/AKT/mTOR signaling pathway. Oncotarget 7: 76827-76839.